SENSITIVITY ANALYSIS OF THE SURFACE ENERGY BALANCE ALGORITHM FOR LAND (SEBAL)

J. Wang, T. W. Sammis, V. P. Gutschick, M. Gebremichael, D. R. Miller

ABSTRACT. *New versions of evapotranspiration (ET) algorithms based on the Surface Energy Balance Algorithm for Land (SEBAL) are being published, each containing slightly different equations to calculate the energy balance. It is difficult to determine what impact changing one or more of the equations or coefficients in the series of equations of SEBAL has on the final calculation of ET. The objective of this article is to conduct a sensitivity analysis of ET estimates in SEBAL to identify the most sensitive variables and equations. A remote sensing ET model based on SEBAL was programmed and validated against eddy-covariance data. A sensitivity analysis was conducted for three contrasting land surface conditions: full, half, and sparse canopy cover in pecan orchards. Results were most sensitive to the selection (according to temperature) of the dry (~zero ET) reference pixel and to c (the estimated ratio of soil heat flux to net solar radiation). At all the three degrees of canopy cover, estimated ET changed by 40% to 270% (1 to 2 mm d^{-1}) when either variable changed from its baseline value by ±50% of the permissible range. Estimated ET was also sensitive to the selection of the wet (full ET) reference pixel and to dT (aerodynamic difference of air and land temperatures). Changes in ET estimates were 47% to 72% (1.3 to 3.7 mm d^{-1}) at both the full and half canopy areas under changes from baseline values equal to 50% of the permissible range for either variable. In addition, ET was sensitive to the roughness length in areas of half canopy cover (ET changed by 61% [1.5 mm d^{-1}]) and to the value of the normalized difference vegetation index (NDVI) in areas of sparse canopy cover (ET changed by 118% [0.35 mm d^{-1}]). Future research on ET algorithm improvement should focus on the above variables and relative equations. The selection of the wet- and dry-spots should be automated to avoid subjective errors from manual selection.*

Keywords. *Energy balance algorithm, Evapotranspiration, Remote sensing, SEBAL, Sensitivity analysis.*

Different models have been developed to estimate evapotranspiration (ET) with extensive spatial coverage based on satellite data (Courault et al., 2003; Gowda et al., 2007). Most of the models require accurate land surface temperature data, which are difficult to obtain. The Surface Energy Balance Algorithm for Land (SEBAL), developed by Bastiaanssen et al. (1998), overcomes this problem by using two anchor pixels (wet and dry, high and low ET) and linearly relating the difference between surface and air temperatures to surface temperature. This feature makes SEBAL a popular choice for operational applications.

The key input data for SEBAL consist of local weather data (wind speed, humidity, solar radiation, and air temperature) and satellite radiance data (visible, near-infrared, and thermal infrared portions of the spectrum). The net shortwave radiation and the soil heat flux are calculated from the radiance data. The sensible heat flux (H) is calculated by assuming a linear relationship between dT (the difference between surface temperature and air temperature) and the surface temperature estimated from thermal infrared radiance. (The Appendix lists all the variable symbols used in this article.) Data from the two anchor pixels (wet and dry) are used to determine the slope and intercept of the linear relationship. Finally, ET is solved as the residual of the energy balance equation.

The initial publication of the SEBAL algorithm consisted of a series of equations that were applied to every pixel in the satellite image. Since then, other researchers have published modifications of the equations used in SEBAL. Allen et al. (2007a) published a model, Mapping Evapotranspiration with Internalized Calibration (METRIC), modifying SEBAL to relieve the assumption that the sensible heat flux (H) is zero at the wet pixel. METRIC calculates H as the energy residual at the pixel, and sets latent heat flux at the cold reference pixel equal to $1.05ET_{r\text{-}h}$, where $ET_{r\text{-}h}$ is the hourly alfalfa reference ET. This latter value is calculated using the standardized ASCE Penman-Monteith equation applied to local meteorological observations. METRIC calculates ET over the dry pixel using a daily surface soil water balance like SEBAL, and calculates daily total ET by multiplying the instantaneous ET by the ratio of the daily alfalfa reference ET to the instantaneous reference ET. Samani et al. (2005a, 2005b) developed the Regional ET Estimation Model (REEM) based on SEBAL, but with different equations for calculating H and net solar radiation (R_n); REEM uses regression equations based on local measured data to compute H

Submitted for review in October 2008as manuscript number SW 7737; approved for publication by the Soil & Water Division of ASABE in May 2009.

The authors are **Junming Wang, ASABE Member Engineer,** Research Scientist, and **Theodore W. Sammis, ASABE Member Engineer,** Professor, Department of Plant and Environmental Sciences, and **Vince P. Gutschick,** Professor, Department of Biology, New Mexico State University, Las Cruces, New Mexico; **Mekonnen Gebremichael,** Assistant Professor, Department of Civil and Environmental Engineering, and **David R. Miller, ASABE Member,** Professor, Department of Natural Resources Management and Engineering, University of Connecticut, Storrs, Connecticut. **Corresponding author:** Junming Wang, Department of Plant and Environmental Sciences, Box 30003, MSC 3Q, New Mexico State University, Las Cruces, NM 88003-8003; phone: 575-646-3239; fax: 575-646-6041; e-mail: wangjunming@hotmail.com.

  ISSN 0001–2351

and R_n. Conrad et al. (2007) used a different strategy to identify the two anchor spots. They combine normalized difference vegetation index (NDVI) and absolute land surface temperature (T_s) to find the anchor spots; high NDVI and low T_s define a wet-spot and low NDVI and high T_s define a dry-spot.

A review of methods to calculate ET using remote sensing energy balance techniques was given by Gowda et al. (2007). For operational purposes of state and federal U.S. agencies, irrigation districts, and engineering firms, SEBAL-type algorithms are most commonly used to calculate ET from remotely sensed data.

There are issues associated with the accuracy of SEBAL or any other satellite-based ET estimation techniques. Errors in satellite-based ET estimates could result from algorithm error, instrumental error, and temporal sampling error. Algorithm errors are directly associated with the approximations to the true physics used to generate estimates of "instantaneous" ET maps. Instrumental errors originate in calibration and measurement noise. Temporal sampling errors arise from infrequent satellite visits and the variability of ET fields in space and time. To minimize potential errors in estimating ET, it is important to quantify the errors and their sensitivity to data and assumed parameter values.

Based on validation results compiled from 18 papers, Bastiaanssen et al. (2005) reported that the accuracy of the SEBAL ET estimates vary from 67% to 95% for instantaneous ET estimates and from 70% to 98% for 1- to 10-day ET estimates. The two worst accuracies were in the studies of Pelgrum and Bastiaanssen (1996) (67% accuracy for instantaneous ET) and Bastiaanssen and Roozekrans (2003) (70% accuracy for 1 to 10 days ET). The factors that affected the accuracies may have been the landscape type, ground measurement method, water stress levels, and climate conditions.

Sensitivity analyses have been conducted on ground-based energy balance algorithms. For example, Bailey and Davies (1981) examined the ET and aerodynamic resistance sensitivity to roughness length and wind speed at a soybean field using ground-based energy balance algorithms. Evaporation estimates from a soybean crop calculated from the model were insensitive to aerodynamic resistance. The resistance was found to be more sensitive to errors in surface roughness than to errors in zero-plane displacement. However, large errors in these had little effect on calculated evaporation. Errors incurred by ignoring atmospheric stability were small in estimating both resistance and evaporation.

Gellens-Meulenberghs (2004) examined the sensitivity of input variables (net solar radiation, R_n; soil heat flux, G; air temperature, T_a; and wind speed, u) and five atmospheric stability functions (Högström, 1988; Brutsaert, 1982; Brutsaert, 1999; Grachev et al., 2000) for a ground-based energy balance algorithm (Royal Meteorological Institute [RMI] Combined Energy Budget-Similarity). The results showed that the stability functions can give large errors (6 to 10 W m^{-2}) for diurnal fluxes (H from 5 to 50 W m^{-2} and latent heat [λET] from 40 to 200 W m^{-2}). Even small standard deviations applied to input data were able to generate important root mean square error values (e.g., 10 W m^{-2}) on both H and λET.

In addition, analyses of the latent heat flux sensitivity to the input data for ground-based energy balance algorithms have been reported (e.g., Stricker and Brutsaert, 1978; Goutorbe, 1991). However, these studies are less comprehensive than that in Gellens-Meulenberghs (2004). The above sensitivity analyses were for ground-based energy balance algorithms.

Sensitivity analysis studies have been performed on SEBAL-like models. For example, sensitivity analyses conducted by Tasumi (2003) on the original SEBAL algorithms showed that doubling or halving the surface roughness parameter did not change the ET estimates by more than 5%. This evaluation was done for a well-irrigated agricultural area, and the results therefore may not be applicable to water-stressed land surface conditions. Crow and Kustas (2005) performed a sensitivity analysis on three parameters, dT, evaporative fraction (EF, hourly ET/daily ET), and r_{ah} (aerodynamic resistance to heat transport), for an energy balance model. They considered sites with different vegetation cover (50% to 90%) at shrub- and grasslands. The EF value did not change with vegetation cover, while dT and r_{ah} were more sensitive to vegetation cover. Their analysis did not go far to quantify ET's sensitivity.

The study presented in this article is a comprehensive study of the sensitivity of SEBAL ET estimates to the input and intermediate variables for land surface conditions under different degrees of vegetation cover (full, half, and sparse) corresponding to various conditions of water availability (no stress, half stressed, and fully stressed) on a summer day in the western U.S. (semi-arid climate and Harkey loam soil).

Materials and Methods

SEBAL-Based RSET Model and Implementation

In this study, we programmed a remote sensing ET (RSET) model, based on SEBAL and written in C++. The model performance was evaluated in Las Cruces, New Mexico. The model simulates ET using data from ASTER (Advanced Spaceborne Thermal Emission and Reflection Radiometer) and local weather stations at a spatial resolution of 90 m × 90 m and a temporal resolution of instantaneous, daily, or longer time scales. ASTER data were obtained from the NASA Earth Observing System Data Gateway (http://redhook.gsfc.nasa.gov/~imswww/pub/imswelcome/). Local weather data consisted of solar radiation, humidity, and wind speed. The RSET model calculates R_n, NDVI, G, and H. As a final step, it calculates the instantaneous ET (λET_{ins}) in W m^{-2}, with ET expressed in energy terms as a residual of the energy balance equation. The instantaneous value is scaled to daily ET flux (λET_{24h}, in W m^{-2}) using the reference crop ET. The ASTER reflectance data have a resolution of 15 m × 15 m for spectral bands 1 through 3 (visible and near-infrared bands) and 30 m × 30 m for spectral bands 4 through 9 (shortwave infrared bands). The ASTER surface temperature data have a resolution of 90 m × 90 m. The reflectance data were linearly averaged over 90 m × 90 m to match the surface temperature data resolution. Each satellite scene covers an area of 60 km × 60 km. The main equations and parameters involved in the RSET model are discussed below.

The model uses the energy budget equation to calculate λET_{ins} over each pixel at the satellite overpass time:

$$\lambda ET_{ins} = R_n - G - H \quad (1)$$

where R_n is the net radiation, computed as the sum of shortwave (R_{ns}, W m^{-2}) and longwave (R_{nl}, W m^{-2}) components:

$$R_n = R_{ns} - R_{nl} \quad (2)$$

A positive sign indicates radiation coming into the surface, while a negative indicates radiation leaving the surface. The R_{ns} is obtained using the incoming solar radiation (R_s, W m^{-2}) measured at the local weather station and surface albedo (γ):

$$R_{ns} = (1-\gamma)R_s \quad (3)$$

Albedo is estimated from the ASTER surface reflectance data using the following equation (Liang, 2000):

$$\gamma = 0.484\alpha_1 + 0.335\alpha_3 - 0.324\alpha_5 + 0.551\alpha_6 + 0.305\alpha_8 - 0.367\alpha_9 - 0.0015 \quad (4)$$

where α_i is the reflectance in spectral band i of the ASTER satellite sensors. The respective bands are visible near-infrared for bands 1 and 3 and shortwave near-infrared for bands 5, 6, 8, and 9, respectively. The symbol R_{nl} is estimated using the regression equation developed by Walter et al. (2002):

$$R_{nl} = 277.8\sigma T_s^4\left(0.34 - 0.14\sqrt{e_a}\right) \quad (5)$$

where T_s is the mean absolute surface temperature (K) as obtained from ASTER thermal infrared data, σ is the Stefan-Boltzmann constant (2.042×10^{-10} MJ K^{-4} m^{-2} h^{-1}), and e_a is the actual water vapor pressure in air (kPa). The value of e_a is obtained from:

$$e_a = \frac{\mathrm{RH}}{100} e_s(T_a) \quad (6)$$

where $e_s(T_a)$ is the saturation vapor pressure (kPa) at air temperature T_a (K), and RH is the relative humidity (%). The $e_s(T_a)$ is calculated from Murray (1967):

$$e_s(T_a) = 0.6108 \exp\left[\frac{17.269(T_a - 273)}{T_a - 35.86}\right] \quad (7)$$

$$\text{with } T_a = T_s - dT \quad (8)$$

where dT is the difference between surface temperature and air temperature (see eq. 16).

The soil heat flux, G, is estimated as a fraction of the net radiation:

$$G = c \times R_n \quad (9)$$

This fraction varies with vegetation cover, which is estimated in SEBAL using NDVI. Using values of NDVI, G, and R_n reported in the literature (Clothier et al., 1986; Choudhury, 1989; Kustas and Daughtry, 1990; Van Oevelen, 1991), we obtained the following functional relationship between c and NDVI (fig. 1):

$$c = -2.70\mathrm{NDVI}^4 + 3.98\mathrm{NDVI}^3 - 1.64\mathrm{NDVI}^2 - 0.11\mathrm{NDVI} + 0.41 \quad (10)$$

These data were obtained over different landscapes (bare soil, sparse vegetation, and full vegetation cover) and under a range of soil moisture levels. For example, Clothier et al. (1986) measured and Choudhury (1989) analyzed c for alfalfa fields over two regrowth cycles during the fall growing season at Phoenix, Arizona. Their data covered a range of vegetative conditions from almost bare soil to full cover by alfalfa of 0.6 m height. Soil volumetric water

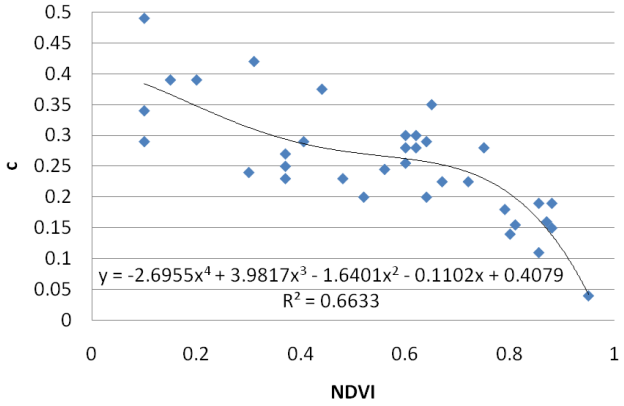

Figure 1. Parameter c (soil heat flux/net radiation) relationship with NDVI (normalized difference vegetation index). Data are from Clothier et al. (1986), Choudhury (1989), Kustas and Daughtry (1990), and Van Oevelen (1991).

content at the surface (0 to 50 mm depth) varied from 0.08 to 0.38. Kustas and Daughtry (1990) measured c during several days near Phoenix for bare, dry soil, alfalfa (0.43 to 0.52 m high, 75% plant cover, saturated water content), and cotton (0.19 to 0.29 m high, 11% to 22% plant cover, 0 to 5 cm surface soil moisture).

NDVI is calculated (Tasumi et al., 2000) as:

$$\mathrm{NDVI} = \frac{\alpha_3 - \alpha_2}{\alpha_3 + \alpha_2} \quad (11)$$

where α_i is the reflectance in spectral band i of the ASTER satellite sensors. Bands 2 and 3 are the bands of visible near-infrared.

The sensible heat flux, H, is computed using wind speed observations, estimated surface roughness, and surface-to-air temperature differences (dT) that are obtained through a self-calibration between dry ($\lambda ET \approx 0$) and wet ($H \approx 0$) pixels, following Bastiaanssen et al. (1998). A dry pixel has no soil water at the surface of a pixel (e.g., dry, bare ground); a wet pixel has enough soil water to attain ET at the reference value (e.g., a well-irrigated crop).

The assumption that $H \approx 0$ at the wet pixel may not be wholly accurate, because there can be modest advection (negative H); air temperature can exceed canopy temperature by several degrees during the daytime (Kalma and Jupp, 1990; Gay and Bemhofer, 1991). However, except over fetch distances somewhat smaller than ASTER pixel sizes between wet and dry surfaces, this heat enhancement of latent heat of ET rarely exceeds the net available energy ($R_n - G$) by 10% (Bastiaanssen et al., 1998). A general assumption of $H \approx 0$ at wet surfaces is therefore a reasonable approximation (Bastiaanssen et al., 1998). In addition, because this study focuses on the sensitivity analysis of SEBAL, we followed the original SEBAL assumption, which is also embedded in most SEBAL-like models.

At the dry pixel, equation 1 reduces to:

$$H = R_n - G \quad (12)$$

Since R_n and G estimates are obtained using equations 2 through 11, H for the dry pixel can be found from equation 12. Using this H, the dT_{dry} value (difference between surface and air temperature at the dry pixel, in

Kelvin) can be found from equations 13 through 15 (Campbell and Norman, 1998):

$$H = \frac{\rho \times c_p \times dT_{dry}}{r_{ah}} \quad (13)$$

where ρ is the air density (mol m^{-3}), c_p is the specific heat of air (29.3 J mol^{-1} °C^{-1}), and r_{ah} is the aerodynamic resistance to heat transport (s m^{-1}). The value of r_{ah} is expressed as:

$$r_{ah} = \frac{\ln(z_2 / z_1)}{u^* k} \quad (14)$$

where z_1 (m) is the zero plane displacement height, z_2 (m) is the reference height above the plant canopy, u^* is the friction velocity (m s^{-1}), and I is the von Karman constant (0.4). The value of u^* is expressed as:

$$u^* = \frac{u(z)k}{\ln[(z-d)/z_m]} \quad (15)$$

where $u(z)$ (m s^{-1}) is the wind speed at reference height z, d (m) is the zero plane displacement height, and z_m (m) is the roughness length.

Following Bastiaanssen et al. (1998), we then assume a linear relationship between dT and T_s:

$$dT = \left(\frac{dT_{dry} - dT_{wet}}{T_{s-dry} - T_{s-wet}}\right) \times T_s - \left(\frac{dT_{dry} - dT_{wet}}{T_{s-dry} - T_{s-wet}}\right) \times T_{s-wet} \quad (16)$$

Once dT is calculated for every pixel in this way, the corresponding H is calculated using equations 13 to 15. The additional variables needed to calculate H from equations 13 to 15 are z_1, z_2, $u(z)$, z, d, and z_m. The values of z_1 and z_2 are set to constant values of 0.1 and 2.0 m, respectively, independent of cover type.

A local weather station provides values of $u(z_0)$ at the measurement height $z = z_0$. The values of d and z_m are known from the cover type at the station. Then u^* can be solved by equation 15. The value of u (at z = 200 m) at other pixels is calculated based on equation 15 using the calculated u^*, and it is applied uniformly across all pixels. The value of d is set to 0 at other pixels, which is a reasonable assumption when z = 200 m. The z_m for each pixel is estimated using a locally calibrated power-law regression between z_m and NDVI, following Tasumi et al. (2000). The calibration of this regression requires at least three pairs of (z_m, NDVI) observations. The equation is empirical and does not have much physical meaning. The regression equation was generated from measured canopy heights (h, using $z_m = 0.1h$) and NDVI data calculated from an ASTER scene of 4 September 2002: z_m = 1.2 m and NDVI = 0.57 for pecan, z_m = 0.07 m and NDVI = 0.42 for alfalfa, and z_m = 0.003 m and NDVI = 0.18 for a bare agricultural field. The z_m values for pecan and alfalfa are calculated as 0.1 multiplied by the plant heights, following Campbell and Norman (1998). The z_m value for bare soil was also from Campbell and Norman (1998). Figure 2 displays the observations and the fitted regression equation.

The equations shown above to estimate H are valid for neutral atmospheric conditions, and appropriate corrections must be applied when the atmospheric conditions are far from neutral. Figure 3 shows the flowchart of the correction. In the stability parameter, or the so-called Monin-Obukhov length, L (m) is calculated from Stull (2001):

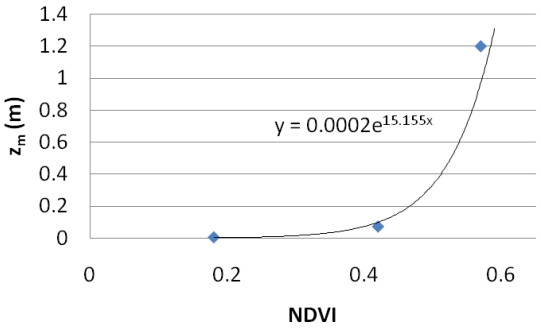

Figure 2. Relationship between z_m (roughness length) and NDVI (normalized difference vegetation index).

$$L = -\frac{u^{*3} T_s}{kgH} \quad (17)$$

where u^* is the friction velocity, T_s is the surface temperature, k is the von Karman constant (0.4), and g is the acceleration of gravity. When $L < 0$, H is positive and heat is transferred upward under unstable conditions; when $L > 0$, H is negative and heat is transferred downward under stable conditions; when L is close to $\pm\infty$, no heat flux occurs under neutral conditions. The stability correction is an iterative process that goes on until H converges (i.e., within 1%). The error in H will cause an error in ET. Because the convergence was within 1%, it will not affect the sensitivity analysis much.

The correction term for stability follows Campbell and Norman (1998) and Stull (2001). The correction may not be appropriate for sparse canopies because the equations for

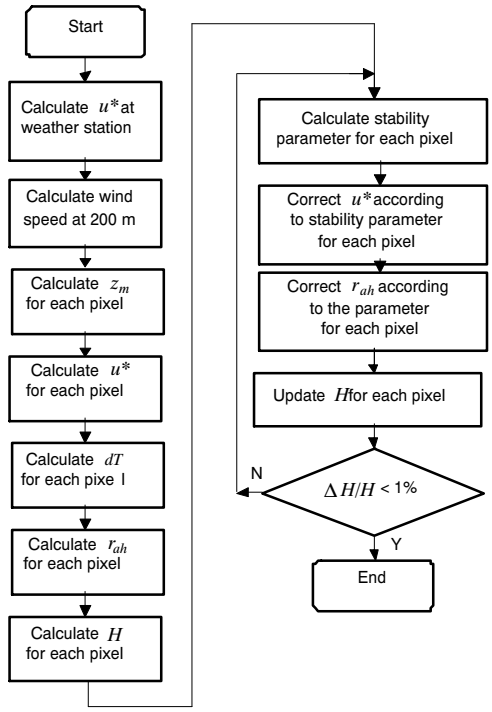

Figure 3. Flowchart of atmospheric correction for sensible heat flux (H) (symbols are defined in the Appendix).

stability correction and sensible heat flux are for homogenous vegetation conditions (Campbell and Norman, 1998; Chehbouni et al., 1994; Crow and Kustas, 2005; Diak et al., 2004; Schmugge et al., 2002; Shuttleworth, 2007; Verhoef et al., 1997). However, calculating ET from soil and canopy separately is difficult (Shuttleworth, 2007). Furthermore, some studies showed that the two-source models (separate soil and vegetation) may not outperform the one-source model (SEBAL) under certain conditions (e.g., vegetated areas) (Crow and Kustas, 2005; French et al., 2005; Wang et al., 2007b). Wang et al. (2007b) compared RSET simulations to sparsely vegetated pecan orchards (3% to 50% vegetation cover), and the results showed that the model is quite accurate (accuracy >90%).

Once the stability-corrected H value is estimated, the next step is to solve for λET_{ins} for each pixel using equation 1. The λET_{ins} is then scaled to the daily time scale using the following relationship (Allen, 2007a, 2007b):

$$ET_{24h} = ET_{r-24h} \frac{\lambda ET_{ins}}{\lambda ET_{r-ins}} \quad (18)$$

where the subscript r refers to the reference crop, in this case well-irrigated alfalfa (i.e., $\alpha = 0.23$, $c = 0.04$, and $T_s = T_{s\text{ - }wet}$). The symbol $ET_{r\text{-}24h}$ denotes the 24 h (daily) ET for the standard reference surface, a well-irrigated alfalfa field. The $ET_{r\text{-}24h}$ is obtained by the ASCE Penman-Monteith equation (Allen et al., 1998). The quantity $\lambda ET_{r\text{-}ins}$ is the instantaneous λET at the satellite overpass time for a well-irrigated alfalfa field, which is obtained from equations 1 to 9.

Work by Bastiaanssen et al. (2005) supports equation 18 for environmental conditions where soil moisture does not significantly change and advection does not occur. The equation appears valid for diverse values of leaf area index (different vegetation cover) (Shuttleworth et al., 1989; Brutsaert and Sugita, 1992; Nicols and Cuenca, 1993; Kustas et al., 1994; Crago, 1996; Franks and Beven, 1997; Farah,

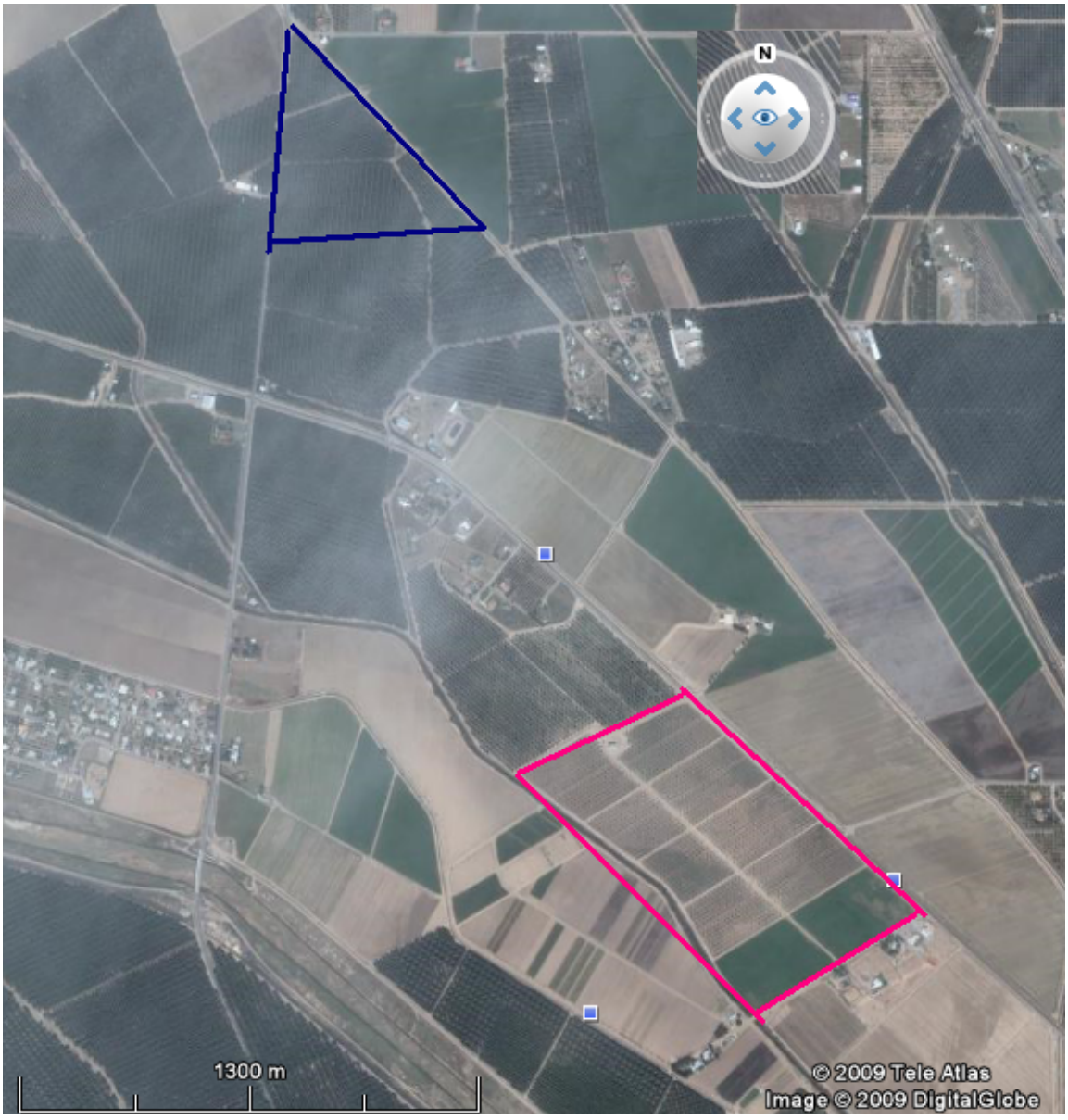

Figure 4. Crop area and the measurement sites in Las Cruces, New Mexico: pecan orchard (triangular area, 32° 13′ 32.45″ N, 106° 45′ 21.75″ W) and alfalfa field (rectangular area, 32° 12′ 20.46″ N, 106° 44′ 27.15″ W). The picture is from Google Earth. ′

2001). In addition, experimental data in Tasumi (2003) indicate that equation 18 is valid for dry, bare ground soil and sugar beet and grass fields.

Experimental Site and ET Measurements

This study was conducted at the Las Cruces pecan crop study area, located in southern New Mexico (fig. 4). It is a semiarid area with a summer monsoon that delivers 55% of the annual precipitation of 250 mm. Potential ET of 2300 mm far exceeds precipitation. Mean annual temperature is 15°C; average monthly highs vary from 13.9°C in January to 34.4°C in June. The soil is Harkey loam (coarse-silty, mixed, calcareous, thermic Typic Torrifluvents). The fields were flood irrigated (≈ 10 cm each irrigation) every two weeks during the growing season.

The pecan orchard (triangular, with sides of 520, 430, and 390 m) was planted in 1970 at a 10 m × 10 m tree spacing. About 2.5 km southwest of the pecan orchard is an alfalfa field (940 m × 530 m). Eddy-covariance instruments (LI-7500 open path CO_2/H_2O gas analyzer, LI-COR, Lincoln, Neb.) were placed in both fields. Flux measurements were conducted from 2002 through 2004. Applying standard eddy-covariance methodology (the covariance of vertical wind velocity and vapor concentration as the vapor flux) described in Wang et al. (2007a), the daily ET values were calculated from these eddy-covariance measurements as 30 min averages and with summation to 24 h ET. A footprint model (Schuepp et al., 1990) was run to ensure that the measured fluxes originated primarily from the study areas. At both the pecan and alfalfa sites, over 95% of the flux was estimated to come from within the uniform crop area.

Validation Statistics

To evaluate the uncertainty in RSET estimates, a comparison is made between RSET estimates and ET observations (as described in the preceding sections). The uncertainty is measured in terms of relative error and absolute error. The relative error is expressed as:

$$\varepsilon_{rel} = \frac{ET_{24h,e} - ET_{24h,o}}{ET_{24h,o}} \quad (19)$$

Table 1. Default conditions for sensitivity analysis (symbols are defined in the Appendix).

	Full Canopy Cover	Half Canopy Cover	Sparse Canopy Cover
α_1	0.099	0.104	0.161
α_2	0.088	0.164	0.184
α_3	0.320	0.322	0.270
α_5	0.138	0.275	0.195
α_6	0.134	0.185	0.276
α_8	0.119	0.158	0.267
α_9	0.199	0.258	0.370
γ	0.147	0.149	0.176
NDVI	0.57	0.31	0.19
T_s (K)	305.7	311.1	320.8
dT (K)	0.9	2.5	5.2
r_{ah} (s m^{-1})	17.6	23.4	19.0
c (G/R_n)	0.27	0.31	0.35
z_m (m)	1.12	0.016	0.003
R_{nl} (W m^{-2})	75	71	67

where the subscripts e and o refer to RSET estimates and ET eddy-covariance observations, respectively. The absolute error is expressed as:

$$\varepsilon_{abs} = \left| ET_{24h,e} - ET_{24h,o} \right| \quad (20)$$

The RSET estimates were compared with measured ET values over two different land covers (alfalfa and pecan) for three scattered dates over alfalfa (17 June 2002, 4 Sept. 2002, and 18 May 2003) and for seven scattered dates over pecan (9 April 2004, 23 April 2003, 4 Sept. 2002, 16 Oct. 2003, 18 May 2003, 7 Sept. 2003, and 17 June 2002). The dates represent different water availability conditions.

The accuracy of the various SEBAL-like algorithms varies from 67% to 95% for instantaneous ET estimates and from 70% to 98% for 1- to 10-day ET estimates (Bastiaanssen et al., 2005). If the average accuracy of a model is above 85%, then it is acceptable, and the average acceptable absolute error (mm d^{-1}) is determined based on the local ET values, e.g., at stressed areas (ET = 2 mm d^{-1}), the acceptable absolute error can be 2 × 15% = 0.3 mm d^{-1}. Therefore, the sensitivity analysis will not produce an average error over 15%.

Sensitivity Analysis

Sensitivity analysis was carried out for three distinct land cover conditions in pecan orchards: 78.5% canopy coverage (full canopy) as projected by crown area (mean NDVI = 0.57), 50% coverage (mean NDVI = 0.31), and 5% coverage in a newly planted orchard (mean NDVI = 0.19). The NDVI values were obtained based on equation 11 from ASTER data from 4 September 2002. Each coverage condition was represented in six pixels, each pixel being 90 m × 90 m. The orchards were all flood irrigated, and the corresponding ET was linearly related to the projected canopy areal coverage (Wang et al., 2007b). Therefore, the three distinct land cover

Table 2. Parameters used in sensitivity analyses at different canopy cover areas (full, half, and sparse) (symbols are defined in the Appendix).

Parameter	Cover	Baseline	Range
Wet-spot selection (temperature, K)	Full	302	294.5-309.5
	Half		
	Sparse		
Dry-spot selection (temperature, K)	Full	322.5	310-335
	Half		
	Sparse		
dT (K)	Full	1.5	0-3.0
	Half	3.0	2.0-4.0
	Sparse	4.5	3.0-6.0
NDVI	Full	0.65	0.5-0.8
	Half	0.35	0.2-0.5
	Sparse	0.15	0.05-0.25
Albedo	Full	0.15	0.05-0.25
	Half	0.175	0.1-0.25
	Sparse	0.3	0.2-0.4
c	Full	0.215	0.03-0.4
	Half	0.32	0.22-0.42
	Sparse	0.4	0.3-0.5
Roughness length (m)	Full	1.25	0.0001-2.5
	Half	1.0	0.0001-2.0
	Sparse	0.5	0.00003-1.0

conditions represent a large range of H/ET values (from 0 when H is 0 to infinity when ET was close to 0).

A summer satellite data set from 4 September 2002 was chosen for this sensitivity analysis. The sensitivity analysis used the following hourly meteorological parameters obtained from the New Mexico State University Climate Center at the Las Cruces Plant Science Research Weather Station (32° 11′ 53.96″ N, 106° 44′ 32.57″ W, elevation 1173 m) at the satellite overpass time: R_s = 800 W m^{-2}, RH = 0.28, $u(z = 2\text{ m})$ = 2.4 m s^{-1}. The other parameters, which vary with land cover conditions, are tabulated in table 1. The sensitivity of ET to various input and intermediate variables was investigated by varying the value of the input or intermediate variables within permissible ranges (table 2). The variables were changed from the baseline values by −50%, −25%, −10%, 0, 10%, 25%, and 50% of the ranges, and the change in estimated ET change was calculated.

Results

Model Performance

An example of the spatial pattern of ET estimated with the RSET model is displayed in figure 5. The figure shows that the ET over the crop area was about 6 mm d^{-1} (red areas) and in the range of 0 to 1 mm d^{-1} over the desert area (black areas). The comparison results are presented in table 3 for alfalfa and pecan fields.

In the alfalfa field, the error of simulated ET was within 2% of the measured ET (0.2 mm d^{-1}) under non-stressed conditions (17 June 2002) and within 6% under water-stressed conditions (4 Sept. 2002, when ET_r was 5.7 mm d^{-1}; and 18 May 2003, when ET_r was 7.1 mm d^{-1}). The average error was 4.3% (average absolute error = 0.23 mm d^{-1}). The alfalfa field had not been irrigated for two weeks prior to the latter two dates, and the alfalfa was 30 cm tall. In the pecan field, the average error of simulated ET was 13% of measured ET (average absolute error = 0.57 mm d^{-1}), and the standard deviation was 8% (0.33 mm d^{-1}). The pecan orchard was always well irrigated. In the spring (April and May) or the end of summer (October), there were low ET values compared with those in mid-summer. The results confirm that the RSET model is accurate within an error of 13%.

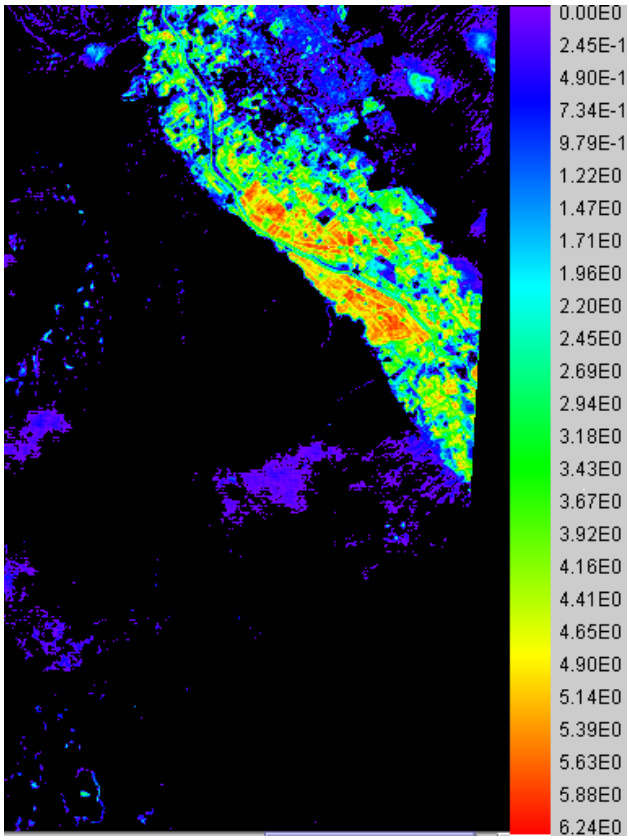

Figure 5. Simulated daily ET (mm d^{-1}) in the Las Cruces, New Mexico, area on 4 September 2002. Resolution: 90 m × 90 m.

Sensitivity Analysis

Figure 6 shows the sensitivity of ET to different variables at different percent canopy cover areas. At the sites of full canopy cover, ET is very sensitive to the wet- and dry-spot selections (temperature values), dT, and c values; ET changes more than 35% with ±50% changes of the permissible range of each variable; and ET is less sensitive to NDVI, albedo, and roughness length (ET changes less than 15%). Among the variables, the selection of a wet-spot has the strongest effect on ET calculations. Selection of an incorrect wet-spot with a temperature of 309.5 K represents a 50% increase from the baseline value of 302 K. Using this to anchor the regression of dT against surface radiative temperature yields a new ET estimate (8.8 mm d^{-1}) that is 72% larger than the baseline value (5.1 mm d^{-1}). The ET output is least sensitive to NDVI. It changes less than 5% if NDVI changes between −50% and 50% (0.5 and 0.8) from the baseline value (0.65). The reason for the small change is that NDVI variation has contrary, nearly cancelling effects on G (c in fig. 1) and H (fig. 7).

At the location with half canopy cover, the ET output is most sensitive to the selection of wet- and dry-spots, roughness length, c, and dT (changes exceeding 35% [1.2 mm d^{-1}] when any of these variables change by ±50%). ET is most sensitive to the selection (temperature) of a dry-spot. A −50% change in the temperature of the dry-spot can result in a −100% change in the ET value. The ET output is least sensitive to NDVI (less than 5% change when NDVI changes by ±50%).

At the area of sparse canopy cover, ET is most sensitive to selection (temperature) of the dry-spot and to c and NDVI. Changes of ±50% in the parameters from their baseline values can result in over 100% change in ET (i.e., >0.7 mm

Table 3. Pecan and alfalfa evapotranspiration (ET) of simulation vs. observation.[a]

	Date	Obs. (mm d^{-1})	Sim. (mm d^{-1})	RE (%)	AE (mm d^{-1})
Pecan	9 Apr. 2004	1.8	2.1	17	0.30
	23 Apr. 2003	4.1	5.1	24	1.00
	4 Sept. 2002	4.5	5.5	22	1.00
	116 Oct. 2003	4.6	4.9	7	0.30
	18 May 2003	5.4	4.7	13	0.70
	7 Sept. 2003	7.7	7.3	5	0.40
	17 June 2002	8.0	8.3	4	0.30
Alfalfa	18 May 2003	4.0	3.8	5	0.20
	4 Sept. 2002	4.7	4.4	6	0.30
	17 June 2002	8.8	8.6	2	0.20

[a] Obs. = ET observation, Sim. = ET simulation, RE = relative error, and AE = absolute error

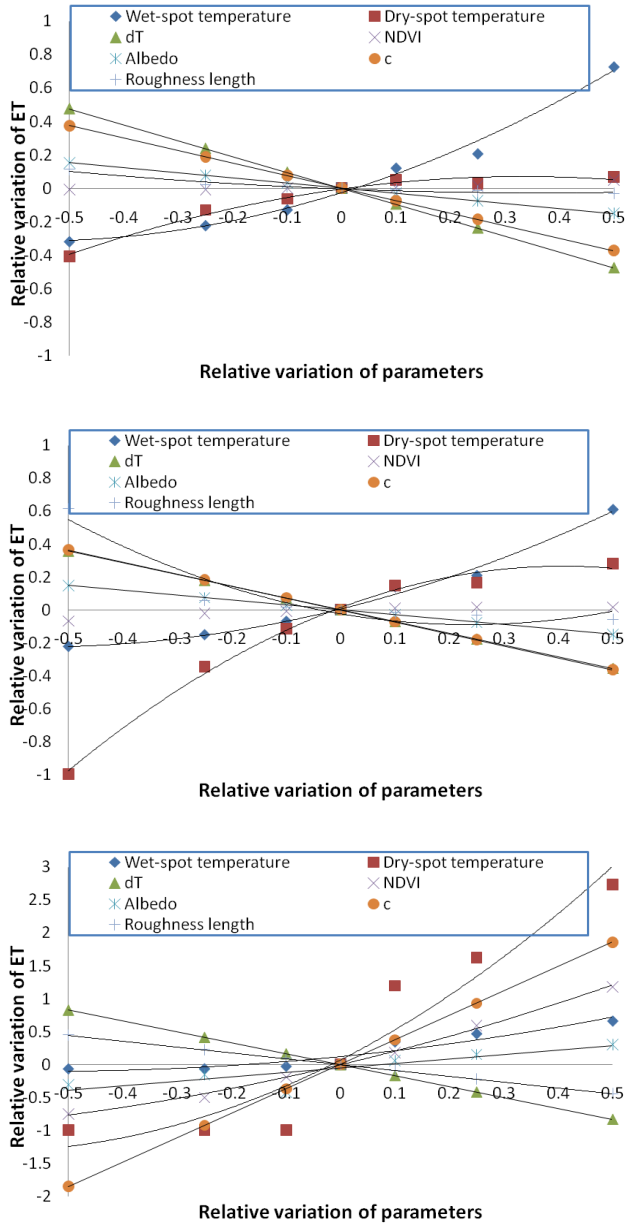

Figure 6. Output of ET sensitivity to the parameters of dry- and wet-spot selection(temperature), difference of air and ground temperature (*dT*), NDVI (normalized difference vegetation index), *c* (soil heat flux/net solar radiation), albedo, and roughness length at areas of full canopy cover (top), half canopy (middle), and sparse canopy (bottom).

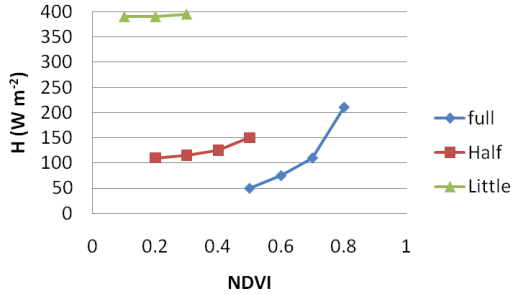

Figure 7. Variable of sensible heat flux (*H*) sensitivity to NDVI (normalized difference vegetation index) at different percent canopy cover areas (full, half, and sparse canopy cover).

d^{-1}). The ET estimate is most sensitive to dry-spot selection, and it can change by 270% (2.6 mm d^{-1}) with a change in dry-spot temperature of 50% from the baseline value 322.5 K. The ET variation with other parameters is less than 0.7 mm d^{-1} over the whole range variation of the parameters (–50% to 50%). The ET value is least sensitive to wet-spot selection and the albedo parameter (less than 0.5 mm d^{-1} change with ±50% variation of the parameter).

Discussion

This study is more comprehensive compared to others in the literature. It examined different vegetation cover areas (with different water stress levels). These study results determined which variables and equations have important effects on the model, and future research should focus on these variables and equations to improve the model. The model has not yet been completely automated, and it requires a technician or researcher to manually download satellite and weather data and process them. The manual operation will prevent some real-time applications. Therefore, model automation is needed. The sensitivity analysis in this study also indicates that, in the automation, much more attention should be paid to certain variables.

This sensitivity analysis study was conducted in the western U.S. However, because the nature of the sensitivity analysis (the output variation with the variable) includes a large value range of the variables, the study results should be applicable to other areas that have different local values for the variables.

The sensitivity analysis in this study was conducted at pecan orchards with different levels of canopy cover. The site-specific parameters of *dT*, *c*, NDVI, roughness length, and albedo were changed over a large value range, which included the possible values from bare ground to grasslands to shrubs to trees. Therefore, the sensitivity analysis should also be applicable to different vegetation covers.

The average accuracy of the RSET model was 87% (average absolute error <0.57 mm d^{-1}) for pecan orchards and 95.4% (average absolute error <0.23 mm d^{-1}) for alfalfa fields. The accuracy is acceptable, and the model is valid for the sensitivity analysis. The sensitivity analysis informs the trend of the effect of one variable variation on the model, and the average error related to the analysis should be smaller than the average error of the model.

The absolute error of T_s does not affect *dT* much if the correct dry- and wet-spots are chosen because *dT* is a relative value calculated from T_s. Any errors in T_s that are constant across pixels or even linear in true T_s are cancelled in the calibration of equation 16. The main problem with all SEBAL-like remote sensing models is determining the appropriate wet-spot (full ET) and the spatial extent over which the resulting regression model can be used in the calculations. Because the wet-spot must represent a location where ET is not limited by soil moisture stress conditions, the ideal site may be hard to find. A nearby lake may be used, but its temperature must be corrected because the lake temperature may be colder than the wet-spot under vegetation cover; advection is common over small lakes.

When using ASTER data, the spatial extent over which SEBAL and similar models can be used is constrained by the size of the scene (60 km × 60 km coverage). This is not a

restriction when using MODIS data for the calculations (2230 km × 2048 km coverage). However, over large areas, the air temperature varies, even as potential temperature. This invalidates a primary assumption of SEBAL. A systematic method of addressing this variation is merited, using spatial statistics, atmospheric circulation models, or both. A related consideration is elevation differences among parts of the scene, especially the wet- and dry-spots. Corrections based on a lapse rate can be used, but the dry adiabatic lapse rate, appropriate for vertical profiles at one horizontal location, may be inappropriate. For example, over arid areas, midday potential temperature (which should be constant in adiabatic conditions) appears to vary consistently with height at all seasons (Andreotti et al., 2009). Additional research is needed. Selecting the dry-spot is simple in the southwestern U.S. because of the desert environment. At other locations in the U.S., a dry-spot may be found from an asphalt area, but the estimation of its aerodynamic resistance is challenging.

The regression equation selection is also a key to the *dT* calculation (eq. 16). Currently, the *dT* equation uses a linear function from T_s. However, a curvilinear relationship may be investigated. Better equations (e.g., those not affected by illumination) for c (G/R_n) calculation also need to be investigated.

The sensitivity analysis shows that the model is very sensitive to the wet- and dry-spot selections. Because the model is manually operated, the model accuracy will partially depend on the operator. Therefore, it is necessary to automate the spot selection process and more objectively select the spots.

The equations for atmospheric stability correction and sensible heat flux calculations were deduced from homogeneous landscapes, and they may not be significantly accurate over areas of partial vegetation cover. Although some research has attempted to resolve the vegetation and soil fluxes separately using two-source models, the results may not be better than SEBAL-like models under certain conditions. For example, the model of Crow and Kustas (2005) demonstrates promise for flux calculations at dry and lightly vegetated sites (bare soil, sparse shrubs, and grasses). However, the results were relatively poor for wet and/or heavily vegetated land surfaces. French et al. (2005) compared SEBAL to measured ET data (eddy-covariance measurements) over sparse areas (soybean fields). The results showed that SEBAL was capable of producing accurate ET with a standard deviation of 1 W m^{-2}, while a two-source model gave a standard deviation of 89 W m^{-2}. Wang et al. (2007b) also compared RSET simulations to ET measurements over sparse pecan orchards (3% to 50% vegetation cover). The RSET model showed an accuracy exceeding 90%. In summary, two-source models may not outperform the one-source model (SEBAL) under certain conditions, and they also increase the complexity of the model development. More research work on remote sensing of ET is needed for sparse vegetation areas.

Conclusion

The energy balance algorithm for remote sensing of ET is sensitive to the selection of the dry-spot and c (G/R_n) value at all the selected areas of full, half, and sparse canopy cover. The estimate of ET is sensitive to the selection of a wet-spot and *dT* at both the full and half canopy cover areas. In addition, ET is sensitive to the roughness length at the area of half canopy cover and sensitive to NDVI at the area of sparse canopy cover.

Improvement of remote-sensing ET algorithms should focus on the above variables and equations. For example, automation should be completed for wet- and dry-spot selections to avoid subjectivity errors. The c function may be improved by eliminating the effects of solar angle and view angle on NDVI (e.g., the corrections for non-Lambertian reflectance; Soenen and Peddle, 2005). For the use of models over large areas, methods must be developed to incorporate the spatial statistics of air temperature in a manner that does not overwhelmingly complicate the models and that is applicable in near real-time.

Acknowledgements

The authors gratefully acknowledge financial support for this research from Southwest Consortium for Environmental Research and Policy, the New Mexico State University Agricultural Experiment Station, the Rio Grande Basin Initiative, and the USDA Forest Service. The authors are grateful to Dr. Tom Schmugge at the Physical Science Laboratory at New Mexico State University for his generous cooperation on satellite data acquisition. The authors thank Mr. Frank Sholedice at University Communications and Marketing Services, Ms. Lyn McKinley at the Department of Agricultural Communications, and Dr. John Mexal at the Department of Plant and Environmental Sciences at New Mexico State University for their great editing work.

References

Allen, R. G., L. S. Pereira, D. Raes, and M. Smith. 1998. Crop evapotranspiration: Guidelines for computing crop water requirements. FAO Irrigation and Drainage Paper No. 56. Rome, Italy: Food and Agriculture Organizations of the United Nations.

Allen, R. G., M. Tasumi, and R. Trezza. 2007a. Satellite-based energy balance for mapping evapotranspiration with internalized calibration (METRIC): Model. *J. Irrig. and Drainage Eng.* 133(4): 380-394.

Allen, R. G., M. Tasumi, A. T. Morse, R. Trezza, W. Kramber, I. Lorite, and C. W. Robison. 2007b. Satellite-based energy balance for mapping evapotranspiration with internalized calibration (METRIC): Applications. *J. Irrig. and Drainage Eng*. 133(4): 395-406.

Andreotti, B., A. Fourrière, F. Ould-Kaddour, B. Murray, and P. Claudin. 2009. Giant aeolian dune size determined by the average depth of the atmospheric boundary layer. *Nature* 457(7233): 1120-1123.

Bailey, W. G., and J. A. Davies. 1981. The effect of uncertainty in aerodynamic resistance on evaporation estimates from the combination models. *Boundary-Layer Meteorol.* 20(2): 187-199.

Bastiaanssen, W. G. M., and H. Roozekrans. 2003. Vlakdekkende actuele verdamping van Nederland operationeel beschikbaar. *Stromingen* 9(4): 5-19 (in Dutch).

Bastiaanssen, W. G. M., M. Menenti, R. A. Feddes, and A. A. M. Holtslag. 1998. A remote sensing surface energy balance algorithm for land (SEBAL). 1. Formulation. *J. Hydrol.* 212-213: 198-212.

Bastiaanssen, W. G. M., E. J. M. Noordman, H. Pelgrum, G. Davids, B. P. Thoreson, and R. G. Allen. 2005. SEBAL model with remotely sensed data to improve water-resources

management under actual field conditions. *J. Irrig. and Drainage Eng.* 131(1): 85-93.
Brutsaert, W. 1982. *Evaporation int*o the Atmosphere: Theory, History, and Applications. Dordrecht, The Netherlands: Kluwer Academic.
Brutsaert, W. 1999. Aspects of bulk atmospheric boundary layer similarity under free convective conditions. *Rev. Geophysics* 37(4): 439-451.
Brutsaert, W., and M. Sugita. 1992. Application of self-preservation in the diurnal evolution of the surface energy balance budget to determine daily evaporation. *J. Geophysical Res.* 97(D17): 18377-18382.
Campbell, G. S., and J. M. Norman. 1998. *An Introduction to Environmental Biophysics.* 2nd ed. New York, N.Y.: Springer Verlag.
Chehbouni, A., J. P. Lhommez, E. G. Njoku, D. Nichols, D. Stannard, S. M. Moran, Y. H. Kerr, and B. Monteny. 1994. Estimation of sensible heat flux using two and three components model during Monsoon '90 experiment. In *Proc. IEEE Intl. Geosci. and Remote Sensing Symp. '94*, 1: 181-183. Piscataway, N.J.: IEEE.
Choudhury, B. J. 1989. Estimating evaporation and carbon assimilation using infrared temperature data: Vistas in modeling. In *Theory and Applications of Optical Remote Sensing*, 628-690. G. Asrar, ed. Hoboken, N.J.: John Wiley and Sons.
Clothier, B. E., K. L. Clawson, P. J. Pinter, M. S. Moran, R. J. Reginato, and R. D. Jackson. 1986. Estimation of soil heat flux from net radiation during the growth of alfalfa. *Agric. and Forest Meteorol.* 37(4): 319-329.
Conrad, C., S. W. Dech, M. Hafeez, J. Lamers, C. Martius, and G. Strunz. 2007. Mapping and assessing water use in a Central Asian irrigation system by utilizing MODIS remote sensing products. *Irrig. and Drainage Syst.* 21(3-4): 197-218.
Courault, D., B. Seguin, and A. Olios. 2003. Review to estimate evapotranspiration from remote sensing data: Some examples from the simplified relationship to the use of mesoscale atmospheric models. In *Proc. ICID Workshop on Remote Sensing of ET for Large Regions*. Denver, Colo.: U.S. Committee on Irrigation and Drainage (USCID).
Crago, R. D. 1996. Comparison of the evaporative fraction and the Priestley-Taylor α for parameterizing daytime evaporation. *Water Resources Res.* 32(5): 1403-1409.
Crow, W. T., and W. P. Kustas. 2005. Utility of assimilating surface radiometric temperature observations for evaporative fraction and heat transfer coefficient retrieval. *Boundary-Layer Meteorol.* 115(1): 105-130.
Diak, G. R., J. R. Mecikalski, M. C. Anderson, J. M. Norman, W. P. Kustas, R. D. Torn, and R. L. DeWolf. 2004. Estimating land surface energy budgets from space: Review and current efforts at the University of Wisconsin-Madison and USDA-ARS. *Bulletin of the American Meteorol. Soc.* 85(1): 65-78.
Farah, H. O. 2001. Estimation of regional evaporation under all sky conditions with satellite and routine weather data. PhD diss. Wageningen, The Netherlands: Wageningen University.
Franks, S. W., and K. J. Beven. 1997. Estimation of evapotranspiration at the landscape scale: A fuzzy disaggregation approach. *Water Resources Res.* 33(12): 2929-2938.
French, A. N., F. Jacob, M. C. Anderson, W. P. Kustas, W. Timmermans, A. Gieske, Z. Su, H. Su, M. F. McCabe, F. Li, J. Prueger, and N. Brunsell. 2005. Surface energy fluxes with the Advanced Spaceborne Thermal Emission and Reflection radiometer (ASTER) at the Iowa 2002 SMACEX site (USA). *Remote Sensing Environ*. 99(1-2): 55-65.
Gay, L. W., and C. Bernhofer. 1991. Enhancement of evapotranspiration by advection in arid regions. In *Hydrological Interactions between Atmosphere, Soil, and Vegetation*, 147-156. G. Kienitz, P. C. D. Milly, M. T. Van Genuchten, D. Rosbjerg, and W. J. Shuttleworth, eds. Wallingford, U.K.: IAHS Press.
Gellens-Meulenberghs, F. 2004. Sensitivity tests of an energy balance model to choice of stability functions and measurement accuracy. *Boundary-Layer Meteorol.* 115(3): 453-471.
Goutorbe, J. P. 1991. A critical assessment of the Samer network accuracy. In *Land Surface Evaporation: Measurement and Parametrization*, 171-182. T. J. Schmugge and J. C. Andre, eds. New York, N.Y.: Springer-Verlag.
Gowda, P. H., J. L. Chávez, P. D. Colaizzi, S. R. Evett, T. A. Howell, and J. A. Tolk. 2007. Remote sensing based energy balance algorithms for mapping ET: Current status and future challenges. *Trans. ASABE* 50(5): 1639-1644.
Grachev, A. A., C. W. Fairall, and E. F. Bradley. 2000. Convective profile constants revisited. *Boundary-Layer Meteorol.* 94(3): 495-515.
Högström, U. 1988. Non-dimensional wind and temperature profiles in the atmospheric surface layer: A re-evaluation. *Boundary-Layer Meteorol.* 42(1-2): 55-78.
Kalma, J. D., and D. L. B. Jupp. 1990. Estimating evaporation from pasture using infrared thermometry: Evaluation of a one-layer resistance model. *Agric. and Forest Meteorol.* 51(3-4): 223-246.
Kustas, W. P., and C. S. T. Daughtry. 1990. Estimation of the soil heat flux/net radiation ratio from spectral data. *Agric. and Forest Meteorol.* 49(3): 205-223.
Kustas, W. P., E. M. Perry, P. C. Doraiswamy, and M. S. Moran. 1994. Using satellite remote sensing to extrapolate evapotranspiration estimates in time and space over a semiarid rangeland basin. *Remote Sensing Environ*. 49(3): 275-286.
Liang, S. 2000. Narrowband to broadband conversions of land surface albedo: I. Algorithms. *Remote Sensing Environ.* 76(2): 213-238.
Murray, F. W. 1967. On the computation of saturation vapor pressure. *J. Applied Meteorol.* 6(1): 203-204.
Nicols, W. E., and R. H. Cuenca. 1993. Evaluation of the evaporative fraction for parameterization of the surface energy balance. *Water Resources Res.* 29(11): 3681-3690.
Pelgrum, H., and W. G. M. Bastiaanssen.1996. An intercomparison of techniques to determine the area-averaged latent heat flux from individual in situ observations: A remote sensing approach using EFEDA data. *Water Resources Res.* 32(9): 2775-2786.
Samani, Z., M. Bleiweiss, S. Nolin, and R. Skaggs. 2005a. Regional ET estimation from satellites. In *Proc. 3rd Intl. Conf. on Irrig. and Drainage*, 613-619. Denver, Colo.: U.S. Committee on Irrigation and Drainage (USCID).
Samani, Z., R. Skaggs, and M. Bleiweiss. 2005b. Regional ET Estimation Model, REEM. In *Proc. 31st Intl. Symposium on Remote Sensing from Satellite*. Tucson, Ariz.: ISRSE.
Schmugge, T. J., W. P. Kustas, J. C. Ritchie, T. J. Jackson, and A. Rango. 2002. Remote sensing in hydrology. *Advances in Water Resources* 25(8-12): 1367-1385.
Schuepp, P. H., M. Y. Leclerc, J. I. MacPherson, and R. L. Desjardins. 1990. Footprint prediction of scalar fluxes from analytical solutions of the diffusion equation. *Boundary-Layer Meteorol.* 50(1-4): 355-373.
Shuttleworth, W. J. 2007. Putting the "vap" into evaporation. *Hydrol. and Earth Syst. Sci.* 11(1): 210-244.
Shuttleworth, W. J., R. J. Gurney, A. Y. Hsu, and J. P. Ormsby. 1989. FIFE: The variation in energy partition at surface flux sites. In *Proc. Workshop Held During the 3rd IAHS Scientific Assembly,* 67-74. A. Rango, ed. Wallingford, U.K.: IAHS Press.
Soenen, S. A., and D. R. Peddle. 2005. SCS+C: A modified sun-canopy-sensor topographic correction in forested terrain. *IEEE Trans. Geosci. and Remote Sensing* 43(9): 2148-2159.
Stricker, H., and W. Brutsaert. 1978. Actual evapotranspiration over a summer period in the "Hupsel Catchment." *J. Hydrol.* 39(1-2): 139-157.

Stull, R. B. 2001. *An Introduction to Boundary Layer Meteorology.* Dordrecht, The Netherlands: Kluwer Academic Publishers.

Tasumi, M. 2003. Progress in operational estimation of regional evapotranspiration using satellite imagery. PhD diss. Moscow, Idaho: University of Idaho.

Tasumi, M., W. G. M. Bastiaanssen, and R. G. Allen. 2000. Application of the SEBAL methodology for estimating consumptive use of water and stream flow depletion in the Bear River basin of Idaho through remote sensing. Final report, EOSDIS Project. Waltham, Mass.: Raytheon Systems Company.

Van Oevelen, P. J. 1991. Determination of the available energy for evapotranspiration with remote sensing. MS thesis. Wageningen, The Netherlands: Wageningen University.

Verhoef, A., H. A. R. De Bruin, and B. J. J. M. Van den Hurk. 1997. Some practical notes on the parameter kB-1 for sparse vegetation. *J. Applied Meteorol.* 36(5): 560-572.

Walter, I. A., R. G. Allen, R. Elliott, D. Itenfisu, P. Brown, M. E. Jensen, B. Mecham, T. A. Howell, R. Snyder, S. Eching, T. Spofford, M. Hattendorf, D. Martin, R. H. Cuenca, and J. L. Wright. 2002. ASCE standardized reference evapotranspiration equation. Reston, Va.: ASCE Environmental and Water Resources Institute, Standardization of Reference Evapotranspiration Task Committee.

Wang, J., D. R. Miller, T. W. Sammis, L. J. Simmons, V. P. Gutschick, and A. J. Andales. 2007a. Energy balance measurements and a simple model for estimating pecan water use efficiency. *Agric. Water Mgmt.* 91(1-3): 92-101.

Wang, J., T. W. Sammis, A. A. Andales, L. J. Simmons, V. P. Gutschick, and D. R. Miller. 2007b. Crop coefficients of open-canopy pecan orchards. *Agric. Water Mgmt.* 88(1-3): 253-262.

APPENDIX

SYMBOLS USED IN THE REMOTE SENSING ET MODEL

c = ratio G/R_n (unitless)
c_p = specific heat of air (J mol^{-1} °C^{-1})
d = zero plane displacement height (m)
dT = difference between surface temperature and air temperature (K)
dT_{dry} = difference between surface temperature and air temperature at a dry-spot (K)
dT_{wet} = difference between surface temperature and air temperature at a wet-spot (K)
e_a = actual air vapor pressure (kPa)
e_s = saturation vapor pressure (kPa)
ET = evapotranspiration (mm d^{-1})
$ET_{24h,e}$ = model-estimated daily ET (mm d^{-1})
$ET_{24h,o}$ = observed daily ET (mm d^{-1})
$ET_{r\text{-}h}$ = hourly alfalfa reference ET (mm h^{-1})
$ET_{r\text{-}24h}$ = daily alfalfa reference ET (mm d^{-1})
g = acceleration of gravity (m s^{-2})
G = soil heat flux (W m^{-2})
H = sensible heat flux (W m^{-2})
K = von Karman constant (unitless)
L = Monin-Obukhov length (m)
NDVI = normalized difference vegetation index (unitless)
r_{ah} = aerodynamic resistance to heat transport (s m^{-1})
RH = relative humidity (%)
R_n = net solar radiation (W m^{-2})
R_{ns} = shortwave solar radiation (W m^{-2})
R_{nl} = longwave solar radiation (W m^{-2})
R_s = incoming solar radiation (W m^{-2})
T_a = air temperature (K)
T_s = absolute land surface temperature (K)
$T_{s\text{-}dry}$ = absolute land surface temperature at a dry-spot (K)
$T_{s\text{-}wet}$ = absolute land surface temperature at a wet-spot (K)
u^* = friction velocity (m s^{-1})
$u(z)$ = wind speed at height z (m s^{-1})
z = height above ground (m)
z_0 = z at height z_0 (m)
z_1 = height of the plant canopy above the zero plane displacement height (m)
z_2 = reference height above the plant canopy (m)
z_m = roughness length (m)
α_i = reflectance in spectral band i of ASTER satellite sensors (unitless)
β = correction variable for the momentum transfer (unitless)
γ = surface albedo (unitless)
ε_{abs} = absolute error (unitless)
ε_{rel} = relative error (unitless)
λET_{ins} = instantaneous latent heat (W m^{-2})
λET_{24h} = daily latent heat (W m^{-2})
ρ = air density (mol m^{-3})
σ = Stefan-Boltzmann constant (MJ K^{-4} m^{-2} h^{-1})
φ = Correction term for the momentum transfer (unitless)